



PREDICTION OF HORIZONTAL RESPONSE SPECTRA OF STRONG GROUND MOTIONS IN IRAN AND ITS REGIONS

H. Sadeghi¹, A. Shooshtari² and M. Jaladat³

ABSTRACT

The large number of strong motion data from the national network of strong motion Iran (NSMNI) motivated this study to develop relations for prediction of response spectra ordinates for periods in the range of 0.1 to 3.0 seconds of horizontal acceleration components of the strong-motion records. We determined attenuation relations of spectral responses to calculate 5% critical damping as a function of spectral periods, and in terms of earthquake magnitude, source to station distance, and recording site conditions. The two horizontal acceleration components of a total of 883 strong-motion records compiled to develop a predictive ground motion model for Iran and its three main seismotectonic regions, Alborz, East and Zagros, and also for the central south of Iran. The data set were recorded from 79 earthquakes from 1987 to 2007, and with moment magnitudes of 5 and larger. A hinged-trilinear form of attenuation model was used for the regression analysis of data set. To estimate the coefficient of attenuation relations we employed the Monte Carlo technique. The results show that while some coefficients are strongly dependent on frequency, some are fairly independent on frequency.

Introduction

The area of the study extends between longitude 44 degrees and 63 degrees east, and between latitudes 25 degrees and 40 degrees north (Fig. 1). The seismotectonic characteristics of Iran are heterogeneous and differ markedly in different regions. Seismicity, earthquake focal mechanisms, and seismotectonic of Iran are discussed by several authors (e.g., Stöcklin, 1968; Nowroozi, 1976; Shoja-Taheri and Niazi, 1981; Berberian, 1983; Sadeghi and Shoja-Taheri, 2006, Engdahl *et al.*, 2008). They introduce the border of seimotectonic regions differently probably related to a markedly different tectonic style in Iran. Although a large quantity of the recorded strong motions by the National Strong Motion Network of Iran is available, a non-uniform distribution throughout Iran limited us to study a predictive ground motion model only for its three distinct tectonic regions; Alborz, East, and Zagros, and also for the central south of Iran.

¹Associate Professor, Earthquake Research Center, Ferdowsi University of Mashhad, Mashhad 9177948974, Iran

²Assistant Professor, Earthquake Research Center, Ferdowsi University of Mashhad, Mashhad 9177948974, Iran

³ Graduated Student, Earthquake Research Center, Ferdowsi University of Mashhad, Mashhad 9177948974, Iran

Strong-Motion Data

A total of 883 two horizontal acceleration time histories from 79 earthquakes of magnitude 5 and higher, were used in this study. The selected earthquakes were recorded by at least three stations within 350 km of epicentral distances. We used the data to develop relations for prediction of response spectra ordinates for periods in the range of 0.1 to 3.0 seconds of horizontal acceleration components of the strong-motion records for the whole of Iran and also for the most active tectonic regions of Alborz, East, Zagros, and Central South. The location of the epicenters and their recording stations is shown in Fig. 1.

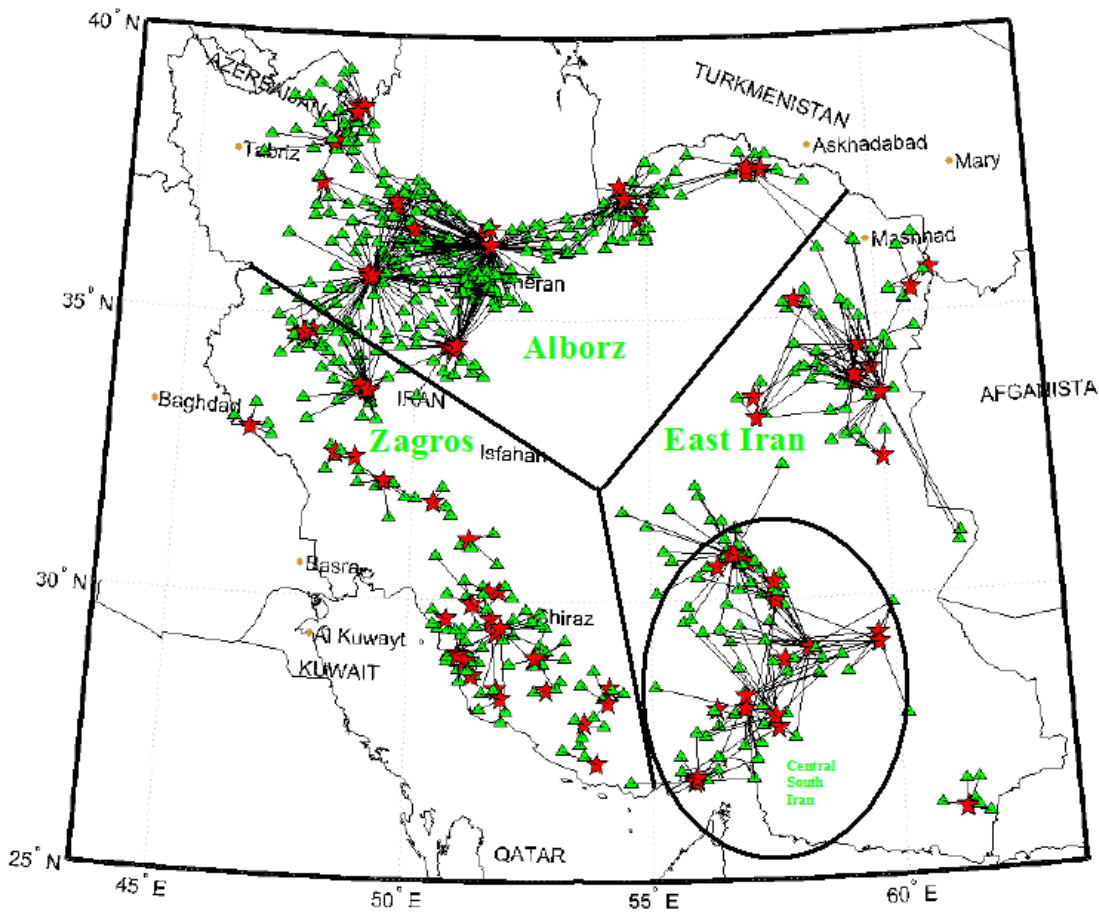


Figure 1. Location Map of the recording stations (573 stations) and epicenters of the earthquakes (79 events). The studied regions of Alborz, East, Zagros, and Central South are shown.

Fig. 2 shows the distribution of the magnitude of the selected events versus distance. The number of selected events and the corresponding number of records for Iran and its regions are listed in Table 1. This table also contains information about the local site condition of the recording stations. The number of records is divided in soil and rock site conditions. We classified the stations into soil and rock classes according to the near surface shear wave velocity

(BHRC- Building and Housing Research Center- database). We used the average S-wave velocity to 30 meters depth, as $V_{s30} < 750$ m/s for soil, and $V_{s30} > 750$ m/s for rock. The H/V method of Nakamura (1989), which is the spectral ratio between the horizontal and the vertical components of strong motions data, also used for the classification of 30 recording stations (see Fig. 3 for an example). We assumed H/V peak frequencies smaller than 7.5 Hz for soil, and greater than 7.5 Hz for rock.

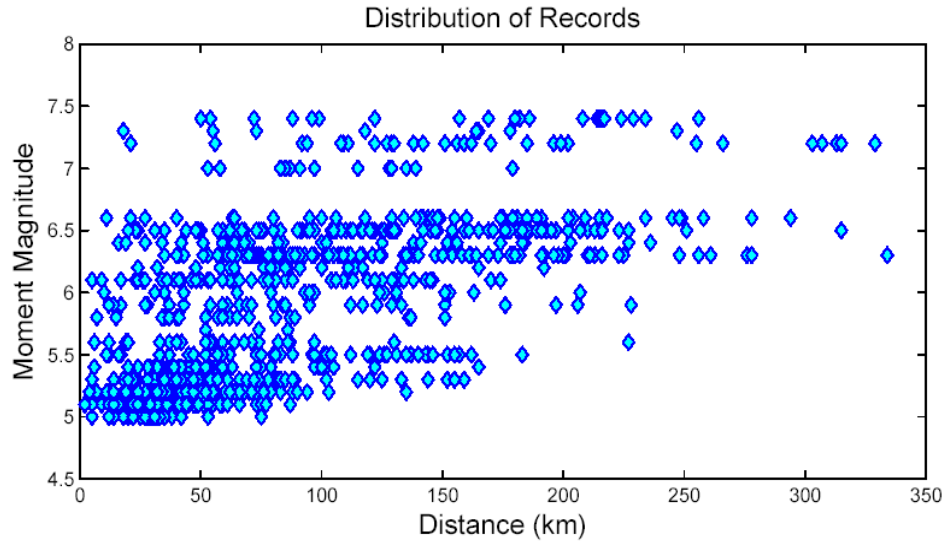


Figure 2. Magnitude-distance distribution of the earthquakes used in this study.

Table 1. Number of Events and Records in different sites and subregions.

No. of	Iran	Alborz	Zagros	East	Central South
Events	79	20	27	32	20
Records	883	423	198	262	175
Rock sites	213	58	68	87	65
Soil sites	556	274	121	161	100

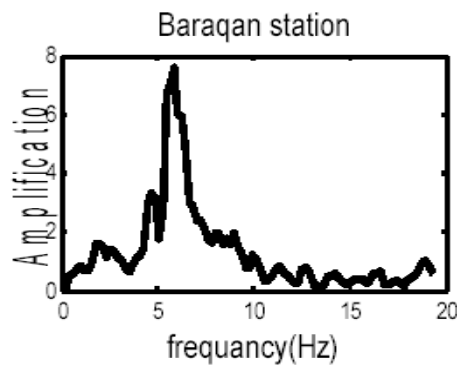


Figure 3. The horizontal-to-vertical spectral ratio (HVSr) at Baraqan Station.

Ground Motion Attenuation Model

A hinged-trilinear attenuation model as the form adopted by Atkinson and Mereu (1992) is used for the regression analysis of the data set in each of three distance ranges:

$$\begin{aligned}
 \log A_{ij}(f) &= a(f) + b(f)M_i - c_1(f) \log R_{ij} - k(f)R_{ij} & R \leq R_1 \\
 \log A_{ij}(f) &= a(f) + b(f)M_i - c_1(f) \log R_1 - c_2(f) \log(R_{ij} / R_1) - k(f)R_{ij} & R_1 < R \leq R_2 \\
 \log A_{ij}(f) &= a(f) + b(f)M_i - c_1(f) \log R_1 - c_2(f) \log(R_2 / R_1) \\
 &\quad - c_3(f) \log(R_{ij} / R_2) - k(f)R_{ij} & R > R_2
 \end{aligned} \tag{1}$$

where A_{ij} is the predicted spectral amplitude for a particular frequency in cm/s^2 for record j of event i , R_{ij} is epicentral distance in km, and M is the moment magnitude. The distances less than R_1 correspond to attenuation of the direct wave. Between R_1 and R_2 is the distance where the direct wave is jointed by postcritical reflections from the Conrad and Moho discontinuities (Burger *et al.*, 1987). The distances beyond R_2 correspond to the multiply reflected and refracted S waves. c_1 , c_2 , and c_3 are the coefficients of geometrical spreading for distances from the source to R_1 , R_1 to R_2 , and beyond R_2 , respectively. k is the coefficient of anelastic attenuation.

Due to the limitation in our data beyond R_2 (see Fig. 2), its geometrical spreading coefficient was considered equal to 0.5. Monte Carlo technique, as used by Izanloo (2005) for eastern Iran, was applied to estimate the coefficients a , b , k , c_1 , c_2 , R_1 , and R_2 . To do this we used a random number generator, tried to find a possible combination of the attenuation parameters by selecting randomly from predefined ranges for each parameter that minimizes the resulting residual errors. The general functional forms of a and b are:

$$a_1 + a_2 \exp(-a_3 T) \tag{2}$$

$$b_1 + b_2 T + b_3 T^2 + b_4 T^3 \tag{3}$$

The results show that coefficients k , c_1 , c_2 , R_1 and R_2 are independent on period, constant coefficient, a , and magnitude coefficient, b , are dependent on period (e.g., Figs. 4, 5, and 6). Izanloo (2005) also obtained the same frequency dependence of the coefficients for eastern Iran. Tables 2 and 3 give the predefined ranges for a and b coefficients and their corresponding function values in Eqs. 2 and 3, respectively. The values for a in table 4 were defined from the functional form of the Eq. 4.

$$a_1 + a_2 T + a_3 T^2 + a_4 T^3 \tag{4}$$

The predefined ranges and mean values for the other coefficients that are independent on period are given in table 5. Using the results listed in the Tables 2 to 5, the attenuation relations of acceleration response spectrum for each region can be derived. Coefficients are to be used for $5.0 < M < 7.5$ and epicentral distance $R < 200$ km. For example, the attenuation relations for east of Iran for all sites are as the following:

For $R \leq 77.2$ km,

$$\log A(T) = (-3.259 + 5.097e^{-0.627T}) + (0.2799 + 0.339T - 0.063T^2)M - 0.825 \log R - 0.0016R \quad (5)$$

For $77.2 < R \leq 117.1$ km,

$$\log A(T) = (-3.259 + 5.097e^{-0.627T}) + (0.2799 + 0.339T - 0.063T^2)M - 0.825 \log 77.2 + 0.0367 \log(R/77.2) - 0.0016R \quad (6)$$

For $R > 117.1$ km,

$$\log A(T) = (-3.259 + 5.097e^{-0.627T}) + (0.2799 + 0.339T - 0.063T^2)M - 0.825 \log 77.2 + 0.0367 \log(117.1/77.2) - 0.5 \log(R/117.1) - 0.0016R \quad (7)$$

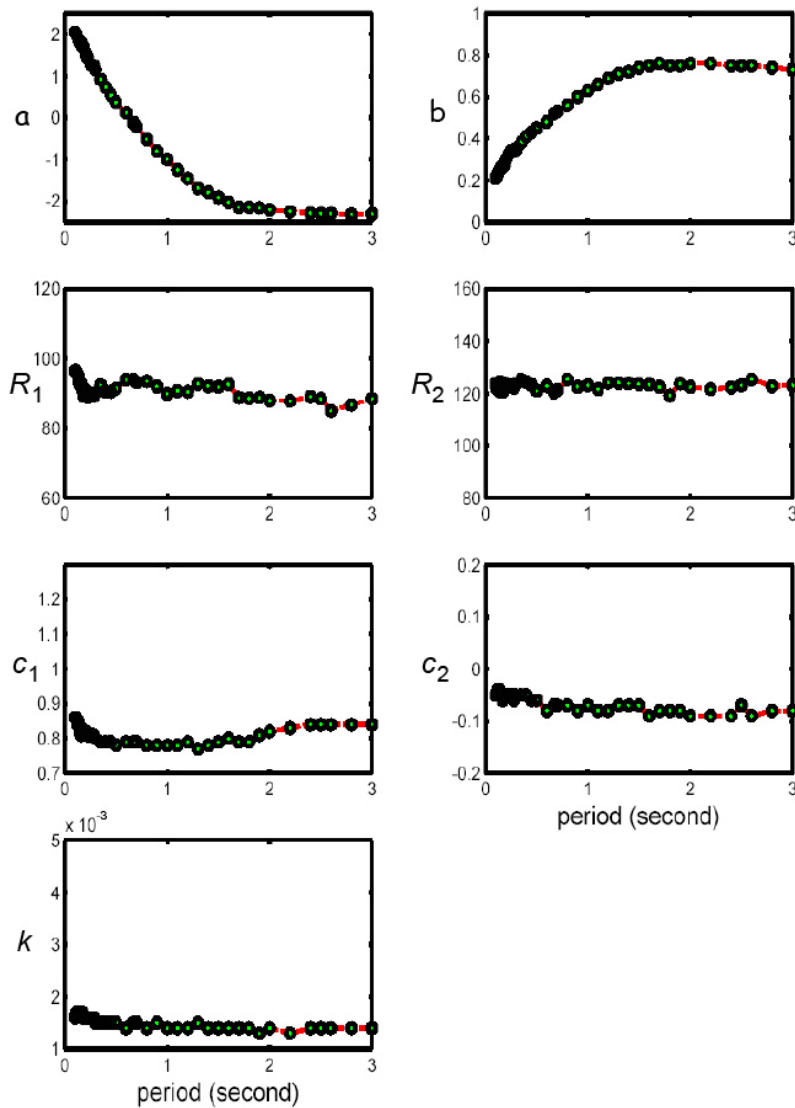


Figure 4. Period dependence of the attenuation coefficients for whole Iran.

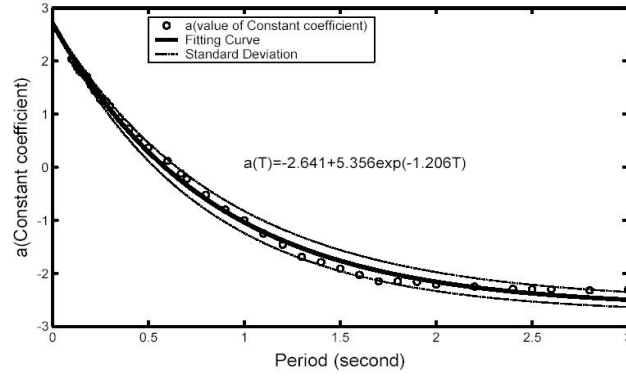


Figure 5. Period dependence of the constant coefficient for whole Iran.

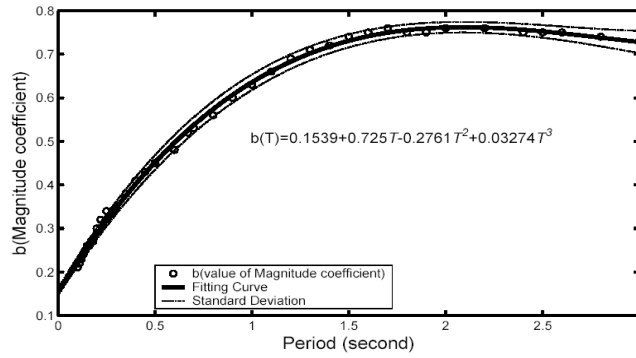


Figure 6. Period dependence of the magnitude coefficient for whole Iran.

Table 2. The predefined range for constant coefficient, a , and their corresponding function values in Eq. 2.

Region	Site	$-2.5 < a < +2.5$					
		a_1		a_2		a_3	
		Mean	SD	Mean	SD	Mean	SD
Iran	All	-2.641	0.110	5.356	0.101	1.206	0.080
	Soil	-2.807	0.194	5.541	0.164	1.015	0.101
Alborz	All	-2.638	0.176	5.799	0.166	1.253	0.127
Zagros	All	-2.432	0.124	5.922	0.174	1.760	0.159
	Soil	-2.452	0.158	5.887	0.193	1.592	0.171
East	All	-3.259	0.326	5.097	0.285	0.627	0.082
	Soil	-4.117	0.814	5.851	0.758	0.432	0.101
Central South	All	-2.867	0.252	4.878	0.211	0.845	0.109
	Soil	-3.954	0.830	5.794	0.765	0.468	0.117

Table 3. The predefined range for constant coefficient, b , and their corresponding function values in Eq. 3.

Region	Site	$0.1 < b < 1$							
		b_1		b_2		b_3		b_4	
		Mean	SD	Mean	SD	Mean	SD	Mean	SD
Iran	All	0.1539	0.0076	0.725	0.030	-0.276	0.025	0.0327	0.0058
	Rock	0.1731	0.0097	0.871	0.038	-0.412	0.032	0.0613	0.0074
	Soil	0.1753	0.0095	0.543	0.020	-0.122	0.007	0	0
Alborz	All	0.0864	0.0101	0.839	0.039	-0.319	0.034	0.0362	0.0070
	Soil	0.0962	0.0147	0.646	0.031	-0.150	0.011	0	0
Zagros	All	0.0462	0.0177	1.170	0.070	-0.611	0.059	0.0996	0.0135
	Soil	0.0488	0.0241	1.098	0.095	-0.554	0.081	0.0884	0.0184
East	All	0.2799	0.0096	0.339	0.020	-0.063	0.007	0	0
	Soil	0.3016	0.0123	0.285	0.026	-0.044	0.009	0	0
Central	All	0.2589	0.0138	0.414	0.029	-0.088	0.011	0	0
South	Soil	0.2827	0.0162	0.311	0.034	-0.050	0.012	0	0

Table 4. The predefined range for constant coefficient, a , and their corresponding function values in Eq. 4.

Region	Site	$-2.5 < a < +2.5$							
		a_1		a_2		a_3		a_4	
		Mean	SD	Mean	SD	Mean	SD	Mean	SD
Iran	Rock	2.350	0.056	-6.031	0.219	2.615	0.188	-0.3773	0.0429
Alborz	Soil	2.924	0.103	-4.566	0.217	0.978	0.079	0	0

Table 5. The predefined ranges and mean values for the coefficient k , c_1 , c_2 , R_1 and R_2 .

Region	Site	$60 < R1 < 120$		$80 < R2 < 160$		$0.7 < c1 < 1.3$		$-0.2 < c2 < 0.2$		$0.001 < k < 0.005$	
		$R1$		$R2$		$c1$		$c2$		k	
		Mean	SD	Mean	SD	Mean	SD	Mean	SD	Mean	SD
Iran	All	91.1	2.6	122.8	1.3	0.810	0.025	-0.0653	0.0161	0.0015	0.00012
	Rock	90.8	2.1	122.6	1.4	0.790	0.021	-0.0565	0.0127	0.0015	0.00007
	Soil	91.4	2.8	122.9	1.2	0.834	0.022	-0.0727	0.0193	0.0015	0.00014
Alborz	All	94.2	3.7	130.2	1.4	0.835	0.018	-0.0817	0.0168	0.0014	0.00011
	Soil	95.9	4.5	130.5	1.4	0.837	0.017	-0.0845	0.0186	0.0014	0.00012
Zagros	All	76.0	2.5	117.6	2.1	0.802	0.046	-0.0687	0.0105	0.0015	0.00010
	Soil	76.2	2.8	117.5	1.6	0.814	0.046	-0.0714	0.0147	0.0015	0.00011
East	All	77.2	0.8	117.1	1.7	0.825	0.018	-0.0367	0.0104	0.0016	0.00009
	Soil	77.7	1.5	117.4	1.6	0.871	0.011	-0.0463	0.0170	0.0016	0.00013
Central South	All	77.8	1.1	117.2	1.5	0.824	0.023	-0.0432	0.0136	0.0016	0.00010
	Soil	78.0	1.2	117.5	1.6	0.884	0.013	-0.0524	0.0183	0.0016	0.00014

The Fig. 7 shows 0.2 second attenuation curves for magnitudes of 5.5, 6.5 and 7.5 in east Iran and Alborz for all sites. We can see three-segment geometrical spreading in these curves, and also clearly presented in other regions and in both soil and rock sites.

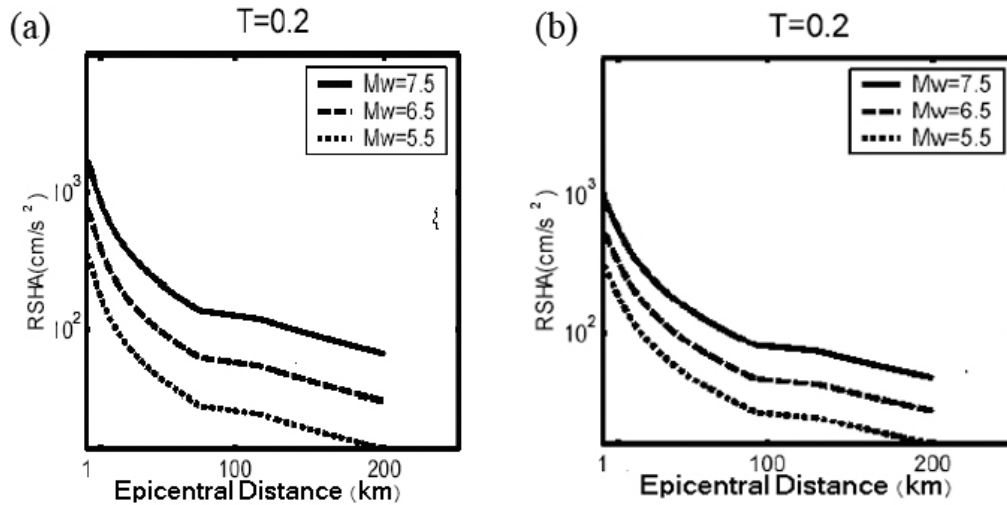


Figure 7. Attenuation curves of the acceleration response spectra for horizontal components (RSHA), (a) east of Iran, and (b) Alborz.

The log residuals of the regression against epicentral distance are plotted in Fig. 8. The log residual is defined as the difference between the log of the observed spectral amplitude and the log of the predicted spectral amplitude. Table 6 shows the logarithmic standard deviation values for the 5%-damped spectral acceleration along with the corresponding periods for Iran.

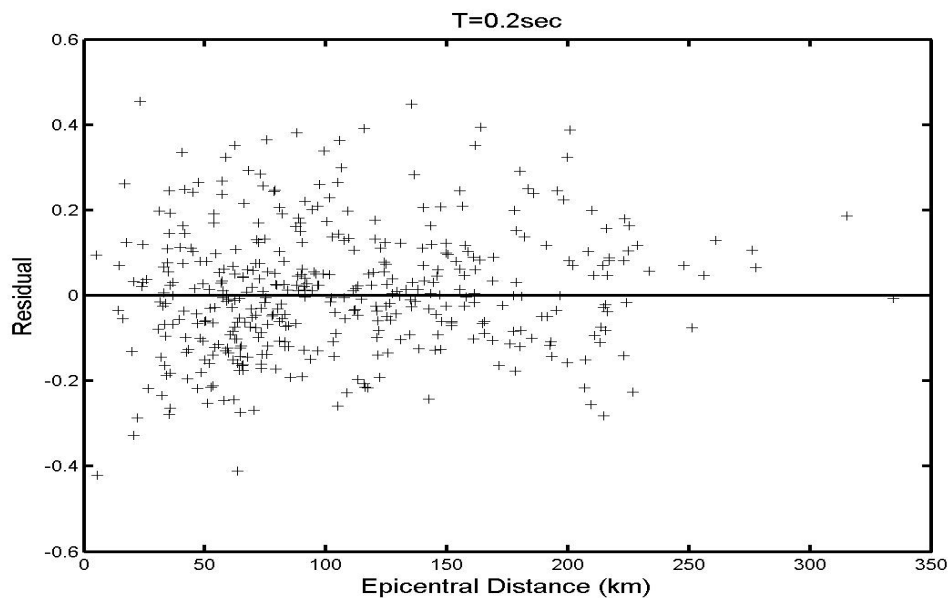


Figure 8. Residuals (log observed – log predicted) versus epicentral distance of 0.2 second spectral amplitude in east of Iran.

Table 6. The standard deviation values of the proposed attenuation model for eight selected periods.

Period	Iran			Alborz		Zagros		East		Central South	
	All	Rock	Soil	All	Soil	All	Soil	All	Soil	All	Soil
0.1	0.27	0.36	0.26	0.31	0.29	0.35	0.37	0.28	0.27	0.27	0.23
0.2	0.24	0.32	0.23	0.27	0.3	0.36	0.36	0.24	0.23	0.24	0.21
0.3	0.28	0.3	0.27	0.3	0.29	0.37	0.36	0.27	0.24	0.27	0.23
0.5	0.25	0.32	0.25	0.3	0.29	0.4	0.41	0.24	0.22	0.23	0.22
1.0	0.28	0.35	0.27	0.37	0.38	0.3	0.31	0.29	0.28	0.29	0.28
1.5	0.27	0.33	0.26	0.37	0.38	0.32	0.33	0.28	0.28	0.27	0.28
2.0	0.26	0.29	0.26	0.31	0.34	0.33	0.33	0.28	0.27	0.27	0.25
3.0	0.25	0.31	0.25	0.25	0.36	0.38	0.37	0.26	0.25	0.29	0.28

The plot in Fig. 9 shows a comparison of predictions of spectral amplitude according to the proposed attenuation relationship, Eq. 1, with that from a standard relationship (Western US). It is seen from the Fig. 9 that the Western US model predicts higher spectral amplitudes than the proposed model for whole Iran.

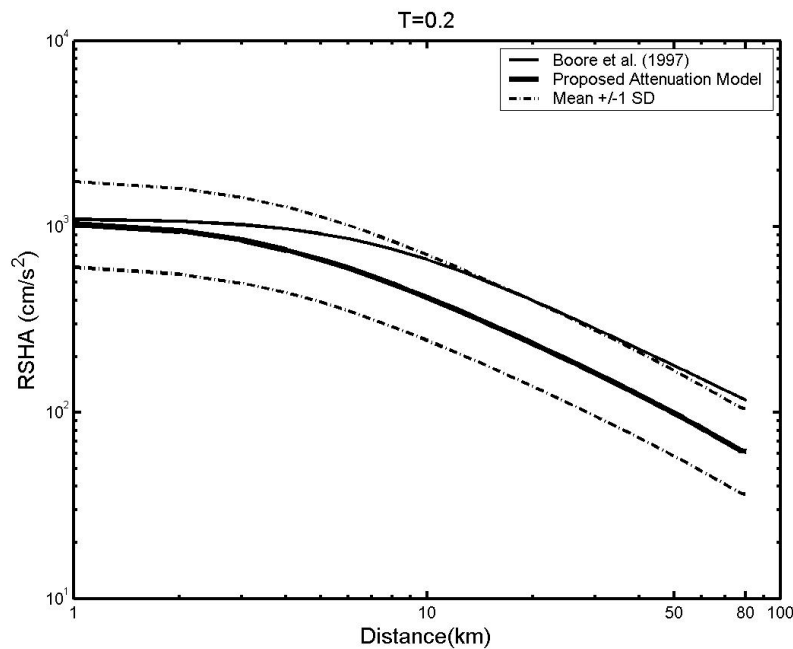


Figure 9. Comparison of predictions from the proposed attenuation model for whole Iran with that from the Western US model for 0.2 second acceleration response spectra for horizontal components (RSHA) for soil and M 6.5.

Conclusions

We developed relations for prediction of 5% damped response spectral acceleration ordinates for periods in the range of 0.1 to 3.0 seconds for Iran and its main seismotectonic regions, using horizontal acceleration components of 883 strong-motion records, from 79 earthquakes during 1987-2007, with moment magnitudes of 5 and larger. The attenuation relations were calculated as a function of period, epicentral distance, and moment magnitude. These include 8 coefficients in which the constant coefficient, and magnitude coefficient are dependent on period and the other coefficients are independent. We can see a three-segment geometrical spreading in the attenuation curves due to direct body waves, the multiply reflected and refracted shear waves from Moho, and surface waves.

Acknowledgments

We thank an anonymous referee for useful comments and suggestions.

References

- Atkinson, G. M., and R. F. Mereu, 1992. The shape of ground motion attenuation curves in southeastern Canada, *Bull. Seism. Soc. Am.* 82, 2014–2031.
- Berberian, M., 1983. *Continental deformation in the Iranian plateau (contribution to the seismotectonics of Iran, part IV)*, Geological Survey of Iran.
- Boore, D. M., Joyner, W. B., and T. E. Fumal, 1997. Equations for estimating horizontal response spectra and peak acceleration from western North American earthquakes: A summary of recent work, *Seism. Res. Letters*, 68, 128-153.
- Burger, R. W., P. G. Somerville, J. S. Barker, R. B. Herrmann, and D. V. Helmberger, 1987. The effect of crustal structure on strong ground motion attenuation relations in eastern North America, *Bull. Seism. Soc. Am.* 77, 420–439.
- Engdahl, E. R., E. A. Bergman, and S. C. Myers, 2008. Seismotectonics of the Iran Region, *American Geophysical Union, Fall Meeting*, abstract #T23D-06
- Izanloo, A., 2005. Attenuation relations for eastern Iran, *MS.c. Thesis*, Ferdowsi University of Mashhad, Mashhad, Iran.
- Nakamura, Y. 1989. A method for dynamic characteristics estimation of subsurface using microtremor on the ground surface, *Rep. Railway Tech. Res. Inst., Jpn.* 30(1), 25-33.
- Nowroozi, A., 1976. Seismotectonic provinces of Iran, *Bull. Seism. Soc. Am.* 66, 1249–1276.
- Shoja-Taheri, J., and M. Niazi 1981. Seismicity of the Iranian plateau and bordering regions, *Bull. Seism. Soc. Am.* 71, 477–489.
- Sadeghi, H., and J. Shoja-Taheri, 2006. Tectonic Stress Indicators in the Iranian Plateau by determining the Focal Mechanism of the Recorded Earthquakes, *Geosciences* (Geological Survey of Iran), 59, 102-119 (in Persian with English abstract).
- Stöcklin, J., 1968. Structural history and tectonics of Iran: a review, *Bull. Am. Assoc. Petrol. Geol.* 52, 1229–1258.